Performance of infrared transmission systems under ambient light interference

A.J.C.Moreira
R.T.Valadas
A.M.de Oliveira Duarte

Indexing terms: Infrared systems, Ambient light interference, Fluorescent lamp interference

Abstract: Optical transmission systems are mainly impaired by the shot noise induced by ambient light, the transmitted optical power limitations (high path losses), the channel bandwidth limitations owing to multipath dispersion and the interference produced by artificial light sources. Several modulation and encoding schemes have been proposed for this channel and their performance has been studied and presented by several authors while neglecting the effects of the artificial light interference. The work reported extends the previous analysis by taking into account the optical power penalty induced by artificial light interference. An analytical approach is used to estimate this. In practical systems, the effect of the interference is usually mitigated using electrical highpass filters. In the paper the combined effect of interference and highpass filter is evaluated. The presented results show that the interference produced by fluorescent lamps driven by electronic ballasts induce high power penalties in OOK and L-PPM systems, even when electrical highpass filtering is used, for data rates up to 10 Mbit/s. For the interference produced by incandescent lamps and fluorescent lamps driven by conventional ballasts, the power penalty induced in OOK systems can be effectively reduced using highpass filtering, while PPM is very tolerant to that interference even without any highpass filtering. The major conclusion is that artificial light interference have to he considered both in system design and performance evaluation.

1 Introduction

Wireless indoor infrared (IR) transmission systems have been used in many applications in the past few years, ranging from simple remote controllers for home appliances to more complex wireless local area networks. The performance of IR transmission systems is impaired by several aspects such as the speed limitations of the optoelectronic devices (LEDs and PIN photodiodes), the high path loss that leads to the requirement for transmission of high optical power levels, the multipath dispersion, the receiver noise, the shot noise induced by the background ambient light and the interference induced by the artificial light sources. From those, multipath dispersion and the background ambient light are the most important sources of degradation.

Multipath dispersion, resulting from multiple reflections of the optical signal on the walls, floor, ceiling and other objects, determines the channel bandwidth as it induces a power penalty on the system performance driven by intersymbol interference (ISI). Typically, its effects are observed for data rates higher than 10Mbit/s [1, 2].

The effects of the background ambient light are observed at all data rates and manifest into two different forms: as shot noise produced in the receiver photodiode, with power proportional to the optical power impinging the photodiode, and as interference produced by the time variations on the intensity of the optical power produced by the artificial light sources. Both the shot noise and the interference produced by the ambient light have been characterised through experimental measurements [3, 4], and it was found that solar light is the most important source of shot noise and that the interference produced by artificial light has different characteristics, intensity and bandwidth, depending on the type of lamp that produces it. In [3], the sources of interference were grouped into three classes: incandescent lamps, fluorescent lamps driven by conventional ballasts and fluorescent lamps driven by electronic ballasts, and it was found that, for this last class, the interference spectrum may extend up to 1MHz.

One of the major technical choices for an IR system is the modulation and/or encoding method. Several schemes have been proposed, some by its simplicity, such as OOK-NRZ and Manchester encoding, and others by its spectral efficiency (N-QPSK, N-BPSK, L-PAM) or by its power efficiency (L-PPM) [1, 5–9]. The performance analysis of these schemes has usually been simplified by reducing the IR channel to an optical additive white Gaussian noise channel (AWGN). These analyses have been extended in [1], where the effects of multipath dispersion were also taken into account. There is, however, evidence that the interference produced by artificial light induces significant power penalties in IR systems [10, 11].

Artificial light interference is usually mitigated by

IEE Proceedings online no. 19960696

Paper received 8th February 1996

The authors are with the Electronics and Communications Department, Universidade de Aveiro, 3810 Aveiro, Portugal

resorting to electrical highpass filtering (HPF), which reduces the effects of the interference but do also introduce some amount of intersymbol interference (ISI). The penalty due to the ISI introduced by HPF have already been evaluated but the penalty induced by the interference itself has not been considered [12, 13].

2 System model

A schematic diagram for an optical wireless transmission system is depicted in Fig. 1. We use three modulation schemes in this paper: OOK-NRZ, L-PPM and BPSK. For each modulation method, one or more information bits a_i are modulated into a symbol and transmitted to the channel. The channel input $X_{in}(t)$ is then used to drive the optical source. At the receiver, the received signal $X_{out}(t)$ (transmitted signal plus noise and interference) is filtered, detected and demodulated to produce an estimate $\tilde{a}_i$ of the original information bits.

In L-PPM, each word of k bits is mapped into one of $L = 2^k$ symbols and transmitted to the channel. An L-PPM symbol has the form of a pulse transmitted in one of L consecutive time slots with duration $T_s = kT_b/L$. Detection of L-PPM symbols requires the estimation of the slot where the pulse was most probably transmitted.

Two detection techniques are considered: threshold detection (TH) and maximum-a-posterior (MAP) or maximum likelihood (ML) detection. The advantage of the TH detector is a lower implementation complexity compared to the MAP detector. In a TH detector, the signal at the filter output is sampled at every L slot and each sample is compared with a threshold. If only one pulse is detected within the L slots, the slot where the pulse is detected is assumed to be the slot where the pulse was transmitted. In the case where more than one pulse is detected, one of those positions may be assumed to be the right one or a position may he assigned at random. In the case where no pulses are detected, one position is assigned at random. In a MAP detector, the signal at the filter output is sampled at every L slot, and the one with the larger sample is assumed to be the right slot. This can be shown to be the optimum detection method for PPM in an AWGN channel [14].

The optical signal transmitted to the channel is produced by modulating the intensity of an optical source, which can be one or more light emitting diodes (LEDs) or laser diodes (LDs). Since channel propagation losses are very high, with values that may be well in excess of 80dB for a typical room [2], arrays of emitting devices are usually used. For low to moderate data rate systems (up to 10Mbit/s), LEDs are a good choice since they are cheaper and require less complex driver circuits than LDs. For higher data rates, LDs may have to he used since LEDs present large rise and fall times, not compatible with the short pulses required for high data rates. In practical systems, the total amount of transmitted optical power and number of emitting devices is limited by cost, size and power consumption considerations and also by the maximum safety levels that are allowed by international standards [15].

In this paper we assume that there are no bandwidth limitations imposed by the optical emitter and that, for OOK and L-PPM, rectangular pulses are transmitted to the channel

$$X_{in}(t) = \begin{cases} 2\,P_{avr} & ,0 \le t < T_b \\ 0 & ,\text{otherwise} \end{cases} \quad (1)$$

for OOK, where P_{avr} is the average transmitted optical power and T_b is the bit period, and

$$X_{in}(t) = \begin{cases} L\,P_{avr} & ,0 \le t < T_s \\ 0 & ,\text{otherwise} \end{cases} \quad (2)$$

for L-PPM, where T_s is the slot period. As the transmitted signal propagates through the channel it is attenuated and dispersion is introduced by the multiple reflections on the walls, ceiling, floor and other surrounding objects, where T_b is the bit duration. In this paper we do not include the effects of multipath dispersion in the performance analysis to evaluate the effects of the interference alone.

At the receiver, the transmitted signal is added to the irradiance produced by the ambient light producing, at the photodetector output, a current given by

$$X_{out}(t) = X_{in}(t) + X_{interf}(t) + I_B + n(t) \quad (3)$$

where $X_{interf}(t)$ is the interference produced by the artificial light (with zero mean), I_B is the DC photocurrent due to the ambient light (natural and artificial), and $n(t)$ is the shot noise produced at the photodiode.

When there is no artificial light, the shot noise is a stationary process. Neglecting the photodetector dark current and assuming that I_B is much larger than the signal current $X_{in}(t)$, the shot noise power spectral density is given by:

$$N_0 \cong q \cdot I_B \quad (4)$$

When there is artifical light, the shot noise is non-stationary and its mean square value at the filter output is given by:

$$\langle n_o^2(t) \rangle \cong q \cdot \int_{-\infty}^{\infty} \{X_{interf}(t) + I_B\} \cdot h_I^2(t-\tau) \cdot d\tau$$

where $h_I(t)$ is the receiver impulse response, including bias circuit, frontend and receiving filter. However, since IB is usually much larger than $X_{interf}(t)$ due to natural ambient light, we have assumed the shot noise to be stationary.

For a well designed receiver front-end, the shot noise generated by the bipolar transistor or FET and the thermal noise are very small compared to the photodetector shot noise and can usually be neglected.

We have characterised the interference produced by

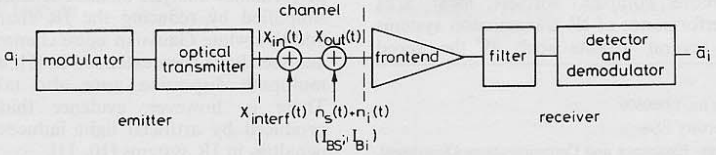

Fig. 1 *Transmission system reference model*

the artificial light [3]. The interference was classified into three classes according to the type of source that produces it: incandescent lamps; fluorescent lamps driven by conventional ballasts and fluorescent lamps driven by electronic ballasts. For each of these classes a model for the interference was proposed and typical values for the model parameters were derived from statistical characterisation of the interference. The major conclusion of that work was that the interference is a periodic and deterministic signal and that the bandwidth of its power spectrum may vary from a few hundreds of Hertz for incandescent lamps to ~1 MHz for fluorescent lamps driven by electronic ballasts.

For OOK-NRZ and L-PPM we assume the use of a matched filter for the rectangular transmitted pulse, assuming a flat power spectral density for the shot noise, i.e. an integrate-and-dump filter. Although not optimum, the same filter is also used in the presence of interference, with and without an highpass filter to block the interference.

3 Channel without interference

In this Section, the performance of NRZ-OOK, L-PPM and BPSK is calculated for a channel without interference but where background shot noise exists owing to natural ambient light.

3.1 OOK-NRZ

For NRZ-OOK, assuming equal probabilities for the '0' and '1' transmitted symbols and that the threshold is set to its optimum value (half the expected filter output at the sampling time), the probability of error P_e is given by

$$P_{e,OOK} = \frac{1}{2} Erfc\left(\frac{P_{avr}\mathcal{R}\sqrt{T_b}}{\sqrt{2N_0}}\right) \tag{5}$$

where P_{avr} is the average transmitted power, N_0 is the noise power spectral density, T_b is the bit period and R is the photodetector responsivity.

3.2 L-PPM

For the TH detector the optimum threshold level that minimises the bit error rate (BER) is a function of the received signal-to-noise ratio (SNR). In practical systems SNR may be difficult to measure, in which case the threshold level is very difficult to set to its optimum level. A reasonable approach is to set the threshold level to a fixed percentage of the signal amplitude. In this case, that percentage must he chosen during the system design phase. The value to choose may he optimised to minimise the BER at low or high values of the SNR. In this paper we assume that the threshold level is half signal amplitude at the sampling time, which approaches the optimum value for high values of the SNR. For low values of the SNR, the BER obtained with this threshold level is always higher than the BER obtained with the optimum threshold.

For the threshold detector, the BER relates to the symbol error rate (SER) by

$$P_{e,PPM\_TH} = \frac{2^{k-1}}{2^k - 1} P_{WS} \tag{6}$$

where P_{WS} is the symbol error probability, given by

$$P_{WS} = 1 - \left(P_1 + \frac{1}{L}P_2 + \sum_{n=2}^{L}\frac{1}{n}P_{3,n}\right) \tag{7}$$

where P_1 is the probability of detection of the pulse at the right position, P_2 is the probability that zero pulses are detected and $P_{3,n}$ is the probability that n pulses are detected, including the right one:

$$P_1 = (1 - P_{01})(1 - P_{10})^{L-1} \tag{8a}$$

$$P_2 = P_{01}(1 - P_{01})^{L-1} \tag{8b}$$

$$P_{3,n} = \binom{L-1}{n-1}(1 - P_{01})P_{10}^{n-1}(1 - P_{10})^{L-n} \tag{8c}$$

where P_{01} is the probability that the right pulse is not detected and P_{10} is the probability that a pulse is detected in a slot where no pulse was transmitted. Assuming that the threshold level is half the expected filter output $P_{01} = P_{10}$ and are given by

$$P_{01} = P_{10} = \frac{1}{2} Erfc\left(\frac{LP_{avr}\mathcal{R}\sqrt{T_s}}{2\sqrt{2N_0}}\right) \tag{9}$$

where T_s is the slot period. For high values of the signal-to-noise ratio P_2 and $P_{3,n}$ became very small, P_{WS} is dominated by P_1 and the bit error rate can be approximated by

$$P_{e,PPM\_TH} \simeq \frac{2^{k-1}}{2^k - 1}\left(1 - (1 - P_{01})^L\right) \tag{10}$$

For the MAP detector, the probability of error (bit error rate) is given by

$$P_{e,PPM\_MAP} = \frac{2^{k-1}}{2^k - 1}(1 - P_{CSC}) \tag{11}$$

where P_{csc} is the probability of correct detection of a symbol [14]

$$P_{CSC} = \frac{1}{\sqrt{\pi}}\int_{-\infty}^{+\infty} \exp(-x^2)\left[\frac{1}{2}\left(1 + Erf(l(x))\right)\right]^{L-1} dx \tag{12}$$

with

$$l(x) = \frac{\sigma_{T_s}x + \frac{v_{T_s}}{\sqrt{2}}}{\sigma_{T_s}} \tag{13}$$

where $v_{Ts} = LP_{avr}RT_s$ is the expected value of the filter output at the sampling time given that a pulse was transmitted and a $\sigma_{Ts}{}^2 = N_0T_s$ is the noise variance also at the sampling time.

3.3 BPSK

For BPSK with coherent detection, the probability of error is given by [14]

$$P_{e,BPSK} = \frac{1}{2} Erfc\left(\frac{P_{avr}\mathcal{R}\sqrt{T_b}}{2\sqrt{N_0}}\right) \tag{14}$$

Results are presented in Section 5 for the relative performance of each of these methods.

4 Channel with artificial light interference

In this Section, the penalty induced by artificial light interference is calculated. The analysis is developed independendy of the type of source that generates the interference. First, the optical power penalty induced by the interference is calculated for the case where no highpass filtering is used, through analytical analysis. Then, the combined effect of the interference and highpass filtering is estimated by simulation. Results are presented in Section 5 for the three types of sources.

4.1 System without highpass filtering

One of the properties of the interference produced by artificial light sources, for all three classes, is that the interfering signal is periodic and deterministic [3]. The properties of the artificial light interference, as described in Section 2, are used in the derivation of closed form expressions for the probability of error in OOK-NRZ and L-PPM systems. For systems using carrier based modulation methods such as BPSK, one can always use a carrier frequency far away from the interference band, thus avoiding the interference signal. This operation may require the use of very high frequency carriers, at which the channel path loss is higher than at lower frequencies [1]. In this sense, the artificial light interference also affects the performance of carrier based modulation methods.

Assuming an integrate-and-dump receiver filter is used, the energy of the interference within the period of a pulse is

$$v_i(t) = \int_{t}^{t+T} X_{interf}(\tau)d\tau \tag{15}$$

where T is the period of the transmitted pulse.

4.1.1 OOK-NRZ: Since the received signal is now corrupted by the interfering signal, one can estimate the probability of error by calculating P_e for each value of the interfering signal and averaging over all values of that interference

$$P_{e,OOK} = \langle P_e(v_i(t))\rangle_{\text{all values of } v_i(t)} \tag{16}$$

Using the fact that the interfering signal is periodic, the probability of error can be estimated by calculating $P_{e,OOK}$ over the period of the interference and averaging over that period:

$$P_{e,OOK} = \frac{1}{T_i}\int_{t_0}^{t_0+T_i}\left[P_0\int_{v_{th}}^{+\infty}P_0(v,v_i(t))dv + P_1\int_{-\infty}^{v_{th}}p_1(v,v_i(t))dv\right]dt \tag{17}$$

where P_0 and P_1 are the probabilities of the '0' and '1' symbols, T_i is the period of the interference and $p_0(v,v_i(t))$ and $p_1(v,v_i(t))$ are the probability density functions of the signal amplitude at the sampling instant, corrupted by the interference $v_i(t)$, given that a '0' or a '1' was transmitted:

$$p_0(v,v_i) = \frac{1}{\sqrt{2\pi}\,\sigma_\tau}\exp\left(-\frac{(v,v_i(t))^2}{2\sigma_\tau^2}\right) \tag{18a}$$

$$p_1(v,v_i) = \frac{1}{\sqrt{2\pi}\,\sigma_\tau}\exp\left(-\frac{(v-(v,v_i(t)))^2}{2\sigma_\tau^2}\right) \tag{18b}$$

where v_T is the expected filter output at the sampling instant, given that '1' was transmitted and v_i is the value of the interference at the sampling time. Assuming $P_0 = P_1 = 1/2$ and $v_{th} = v_T/2$, eqn. 17 takes the form

$$P_{e,OOK} = \frac{1}{T_i}\int_{t_0}^{t_0+T_i}\left[\frac{1}{4}Erfc\left(\frac{P_{avr}RT_b - v_i(t)}{\sqrt{2N_0T_b}}\right) + \frac{1}{4}\left(1+Erf\left(\frac{-P_{avr}RT_b - v_i(t)}{\sqrt{2N_0T_b}}\right)\right)\right]dt \tag{19}$$

4.1.2 L-PPM: For L-PPM, the same approach can he used to derive the expression for the probability of error. As described in Section 3, two methods may he used to detect PPM signals. In this Section those two methods are also considered.

We define the interference in one PPM symbol by the vector $\mathbf{V}(t)$ where each element is the value of the interference at the sampling time for each one of the L consecutive time slots:

$$\mathbf{V}(t) = \{V_i(t), v_i(t+T_s), v_i(t+2T_s), \ldots, v_i(t+(L-1)T_s)\} \tag{20}$$

with $v_i(t)$ given by eqn. 15 with $T = T_s$. For the TH detector, using the same approach as for OOK, we have

$$P_{e,PPM\_TH} = \frac{2^{k-1}}{2^k-1}\frac{1}{T_i}\int_{t_0}^{t_0+T_i}P_{WS}(\mathbf{V}(t))dt \tag{21}$$

The exact expression for $P_{WS}(\mathbf{V}(t))$ is very complex and takes a lot of computation time to evaluate. Fortunately, an upper bound can be determined if we consider as correct symbols those where only the right pulse is detected (as in eqn. 10):

$$P_{WS}(\mathbf{V}(t)) \le 1 - \frac{1}{L}\sum_{k=1}^{L}(1-P_{01}(\mathbf{V}_k))\prod_{\substack{j=1\\ j\neq k}}^{L}(1-P_{10}(\mathbf{V}_j)) \tag{22}$$

where $\mathbf{V}_k$ is the k element of vector $\mathbf{V}$ and

$$P_{01}(\mathbf{V}_k) = \frac{1}{2}\left[1+Erf\left(\frac{-v_T-2\mathbf{V}_k}{2\sqrt{2}\,\sigma_\tau}\right)\right] \tag{23a}$$

$$P_{10}(\mathbf{V}_j) = \frac{1}{2}Erf\left(\frac{v_T-2\mathbf{V}_j}{2\sqrt{2}\,\sigma_\tau}\right) \tag{23b}$$

In Section 5 the results obtained using this upper bound are compared to the results obtained through simulation. For the MAP detector, the BER is given by

$$P_{e,PPM\_MAP} = \frac{2^{k-1}}{2^k-1}\left(1-\frac{1}{T_i}\int_{t_0}^{t_0+T_i}P_{CSC}(\mathbf{V}(t))dt\right) \tag{24}$$

with

$$P_{CSC}(\mathbf{V}(t)) = \frac{1}{L}\sum_{k=1}^{L}\int_{-\infty}^{+\infty}p_{1,k}(x)\left(\prod_{\substack{j=1\\ j\neq k}}^{L}\int_{-\infty}^{x}p_{0,j}(y)dy\right)dx \tag{25}$$

where $p_{1,k}(x)$ is the probability density function of the filter output at the sampling time given that a pulse was transmitted in that slot

$$p_{1,k}(x) = \frac{1}{\sqrt{2\pi}\,\sigma_\tau}\exp\left(\frac{-(x-v_\tau-\mathbf{V}_k)^2}{2\sigma_\tau^2}\right) \tag{26}$$

and $p_{0j}(y)$ is the probability density function of the filter output at the sampling time given that no pulse was transmitted in that slot

$$p_{0,j}(y) = \frac{1}{\sqrt{2\pi}\,\sigma_\tau}\exp\left(\frac{-(y-\mathbf{V}_j)^2}{2\sigma_\tau^2}\right) \tag{27}$$

Substituting eqns. 26 and 27 in eqn. 25 we have

$$P_{CSC}(\mathbf{V}(t)) = \frac{1}{L\sqrt{\pi}}\sum_{k=1}^{L}\int_{-\infty}^{+\infty}\exp(-w^2)$$

$$\times \left(\prod_{\substack{j=1 \\ j \neq k}}^{L} \frac{1}{2} \left(1 + Erf\left[\Phi_{k,j}(w) \right] \right) \right) dw \quad (28)$$

with $\Phi_{k,j}(w)$ a set of functions defined as

$$\Phi_{k,j}(w) = \frac{\sqrt{2}\,\sigma_\tau w + v_T + \mathbf{V}_k - \mathbf{V}_j}{\sqrt{2}\,\sigma_\tau} \quad (29)$$

4.2 System with highpass filtering

Electrical highpass filtering is usually employed to mitigate the effects of the artificial light interference. Since the interference amplitude may be much higher than the signal amplitude, practical systems may have to resort to highpass filtering to avoid saturation of the input stages of the optical receiver, even if the penalty induced by the interference is small. Highpass filtering solves or attenuates the problems described, but also introduces some intersymbol interference. The filter cut-off frequency is a compromise between the attenuation of the interference and the amount of ISI that is introduced.

Depending on the modulation method and type of interference we have used a first order or second order Butterworth highpass filter. In practical systems, this type of filter can he implemented by tuning the AC coupling between successive analogue stages of the receiver, without the need to increase the hardware complexity. In the work reported in this paper, we have used simulation to estimate the combined effects of interference and ISI. All simulations were performed using the software package SPW [16] (Signal Processing Worksystem).

5 Results

The performance of wireless infrared transmission systems is very dependent on the channel characteristics. For each particular room, type, number and position of the illuminating devices, existence or not of natural ambient light, position of the receiver and data rate, the performance of the transmission system will be different. For these reasons we have selected four typical cases of ambient light, with and without interference, to estimate the performance of the transmission systems. The shot noise and interference levels were derived from a statistical characterisation of the ambient light [3]. The four cases of ambient light considered in this work are the following:

Case 1: No interference: natural (solar) light only (I_{Bs} = 200μA)

Case 2: Incandescent interference: natural light plus an incandescent 60W lamp placed 1m away from the receiver, e.g. a desktop light (I_{Bi} = 56μA)

Case 3: Fluorescent interference: natural light in a room also illuminated with fluorescent lamps (8 times 36W in a 5 × 6m room), geared by conventional ballasts, with the receiver placed under one of the pairs of lamps, 2.2m high (I_{Bi} = 2μA)

Case 4: Electronic ballast fluorescent interference: similar to case 3, but with fluorescent lamps geared by electronic ballasts (I_{Bi} = 2μA)

As described in [3], the I_B values are sufficient to characterise both the shot noise and interference levels. The interference waveform $X_{interf}(t)$ for each type of interference was obtained using the model proposed in [3]. In that model, the interfering sources were organised into three classes and a model for each class was derived through statistical characterisation of the model parameters. Using these values the results presented in this Section are also a measure of the performance of the transmission systems operating under typical ambient light noise and interference conditions.

5.1 Channel without interference (case 1)

In Fig. 2, the BER against the received optical power is plotted for OOK-NRZ, BPSK and L-PPM with MAP detection for L = 4, 8 and 16. For this channel, the performance of 2-PPM is equal to that of OOK. A curve for 16-PPM with TH detection is also shown. In all the results the power requirements were normalised to the power required for OOK-NRZ at BER = 10^{-5} in a channel limited by shot noise only.

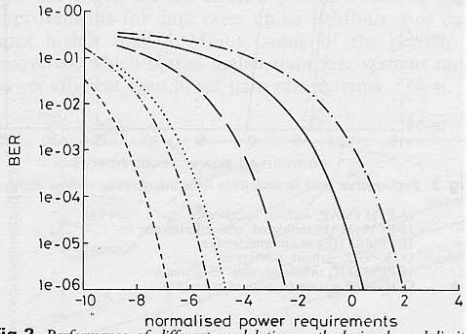

Fig.2 *Performance of different modulation methods in channel limited only by shot noise*
——— OOK-NRZ
– – – – 16-PPM
· · · · · 8-PPM
— — — 4-PPM
— · — · BPSK-coherent
— · — · 16-PPM, TH

Clearly, L-PPM is the most power efficient modulation method. For the shot noise limited channel, the relative performance of each technique is independent of the bit rate since no bandwidth limitations were considered in this paper. Also, for the same reason, the carrier frequency used for BPSK is irrelevant for its performance. For 16-PPM, the TH detector requires about 1.5dB more optical power than the MAP detector for the same BER. For other orders of PPM the difference between the two methods is very similar.

5.2 Channel with incandescent interference (case 2)

Fig. 3 shows the performance of OOK and 16-PPM systems at 1Mbit/s, operating under incandescent interference without electrical highpass filtering (HPF). The lines represent calculated values and simulation results are represented by dots.

For OOK, the penalty is very large, being around 24dB. For 16-PPM with TH detection the behaviour is similar, with a penalty of about 16dB. On the contrary, for 16-PPM with MAP detection the power penalty is very small, being about 1.5dB. This is explained by the fact that for this data rate the interference values at

sampling time in the successive slots within a symbol are very similar, i.e. the elements of vector $\mathbf{V}(t)$ (eqn. 20) are all very similar. Since in a MAP detector a symbol is detected by taking the slot with the larger sample, an interference that adds the same value (or very similar value) to all slots does not affect the performance. The 1.5dB penalty shown in Fig. 3 is mostly due to the additional shot noise introduced by the incandescent light (I_B = 200+56μA). Note that there is a very good agreement between the simulation results and the calculated results, showing that for L-PPM with TH detection the upper bound considered in eqn. 22 provides a good estimate of the system performance.

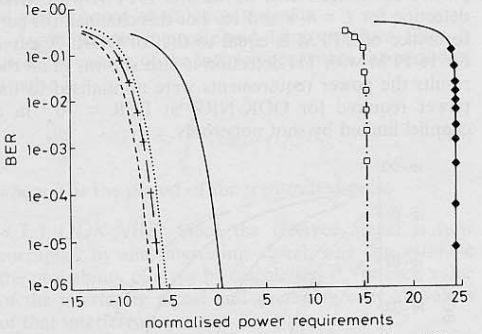

Fig.3 *Performance with incandescent light interference without highpass filtering*
- – – 16-PPM (MAP) without interference
- –+– 16-PPM (MAP) simulated, with interference
- ····· 16-PPM (TH) without interference
- ——— OOK-NRZ without interference
- –□– 16-PPM (TH) simulated, with interference
- —◆— OOK-NRZ simulated, with interference

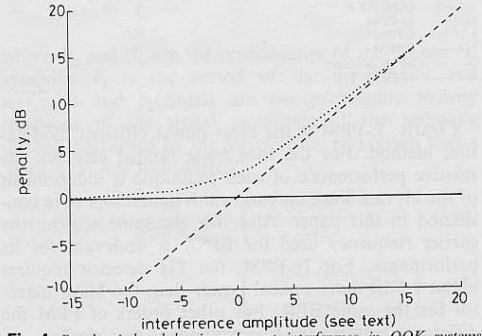

Fig.4 *Penalty induced by incandescent interference in OOK systems against interference amplitude*
- ——— OOK without interference
- – – – interference amplitude
- ····· OOK with interference

In Fig. 4, we compare the penalty induced in an OOK system without HPF with the interference amplitude, calculated as $10\log_{10}(\max[|v_I(t)|]/10^{-3})$ $-P_{arr,BER} = 10^{-5}$ for all values of t over one period of the interference. The main conclusion is that for high values of the interference amplitude, as in case 1, the power requirements are approximately given by the interference amplitude, as defined.

In Fig. 5, results are presented for systems at 1Mbit/s using HPF. The values between parentheses represent the filter cut-off frequency and are approximately the values that provide the best performance, i.e. the values for which the BER is lower.

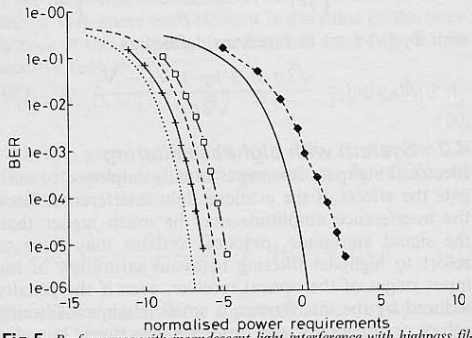

Fig.5 *Performance with incandescent light interference with highpass filtering*
- ——— OOK, no interference
- –◆– OOK, with filter (4kHz)
- – – – 16-PPM, MAP, no interference
- —+— 16-PPM, MAP, with filter (500Hz)
- —·—· 16-PPM, TH, no interference
- –⊡– 16-PPM, TH, with filter (6kHz)

For OOK and 16-PPM with TH detection, HPF effectively reduces the penalty induced by the interference. For 16-PPM with MAP detection, the use of HPF does not provide significant improvements over the system without filtering since the penalty without filtering is already very small and, as stated previously, mostly owing to the additional shot noise.

For systems operating at different data rates the penalties induced by artificial light interference are also different. This is shown in Fig. 6, where the penalty induced by incandescent interference is plotted as a function of the data rate. For OOK and 16-PPM with TH detection without HPF, the power requirements are almost constant for all data rates, from which results a penalty that decreases linearly with the data rate. These large penalties are considerably reduced by resorting to HPF, but for low data rates the penalty is still very large. For 16-PPM with MAP detection, the penalty is very small for data rates higher that 1Mbit/s, even without HPF, and for low data rates (100kbit/s) the penalty can also be made very small by resorting to HPF.

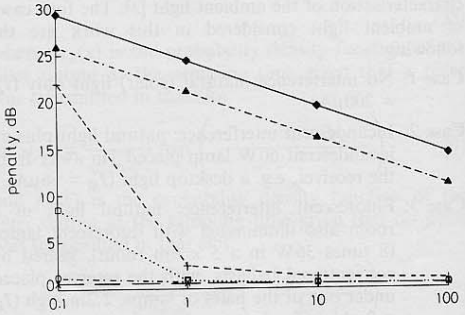

Fig.6 *Power penalty against data rate for incandescent light interference*
- —◆— OOK, no filter
- —+— OOK, with filter
- –□– 16-PPM, MAP, no filter
- –×– 16-PPM, MAP, with filter
- –·▲–· 16-PPM, TH, no filter
- –·×–· 16-PPM, TH, with filter

5.3 Channel with fluorescent interference (case 3)

The effects of the interference produced by fluorescent lamps driven by conventional ballasts are very similar to those produced by incandescent interference, as shown in Fig. 7 for systems of 1 Mbit/s. Using HPF, the penalties induced in OOK and PPM systems with TH detection can be made very small, while for L-PPM with MAP detection the penalty is small even without HPF. The major difference is that the penalty induced by the additional shot noise is almost negligible since fluorescent light produces much lower average irradiance levels than incandescent light.

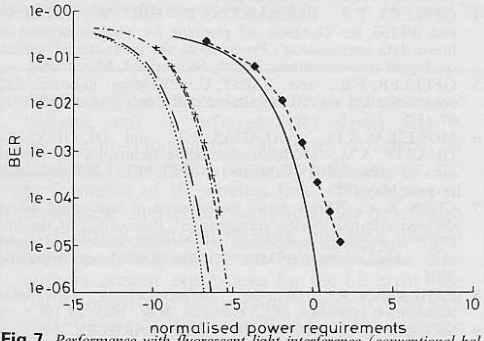

Fig. 7 *Performance with fluorescent light interference (conventional ballast)*
OOK, no interference
OOK, with filter (4 kHz)
16-PPM, MAP, no interference
16-PPM, MAP, with interference
16-PPM, TH, no interference
16-PPM, TH, with filter (6 kHz)

5.4 Channel with interference produced by fluorescent lamps driven by electronic ballasts (case 4)

In a channel with fluorescent lamps driven by electronic ballasts, the performance of the transmission systems is strongly degraded, as shown in Fig. 8 for OOK, 4-PPM and 16-PPM systems operating at 1 Mbit/s.

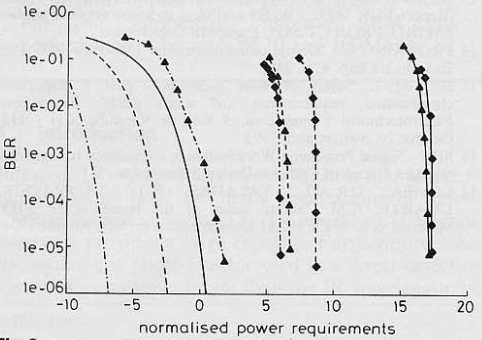

Fig. 8 *Performance with fluorescent light interference (electronic ballast)*
OOK
4-PPM
16-PPM
◆ no filter
▲ with filter

As for the other types of interference, the penalty induced in OOK systems without HPF is very large. However, for this type of interference, HPF does not provide significant improvements in reducing the penalty, making OOK not a practical solution for 1 Mbit/s systems, unless different techniques are used to mitigate the effects of the interference. For L-PPM with TH detection (not shown in Fig. 8), HPF provides better results but, for this case, a penalty in excess of 12dB still remains after HPF.

For L-PPM with MAP detection, the performance with or without HPF is also strongly affected by this type of interference. HPF provides some improvements, but penalties of about 8.9dB (the lower value) are found even for 16-PPM, which is shown to be the better solution.

In Fig. 9 the power requirements for OOK, 4-PPM and 16-PPM (MAP), with and without HPF are shown as a function of the data rate. For OOK without HPF, as for the other types of interference, the power requirements are the same for all data rates up to 100 Mbit/s. This effect results from the dependency of the power requirements on the interference amplitude, as shown in Fig. 4 for the incandescent interference. Also for OOK, the use of HPF provides none or small improvements for data rates up to 10 Mbit/s. For data rates higher than 10 Mbit/s, some of the penalty is recovered, which makes higher data rate systems more power efficient than lower data rate systems.

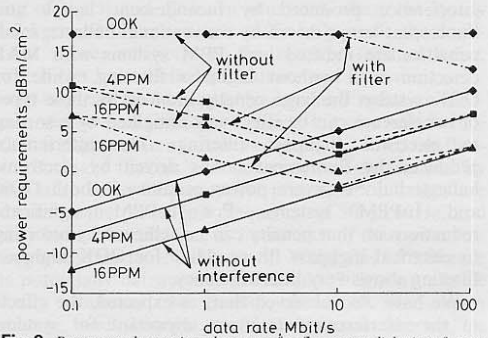

Fig. 9 *Power penalty against data rate for fluorescent light interference with electronic ballast*

With both 4-PPM and 16-PPM, the penalty for low data rates (100 kbit/s) is very large and HPF does not provide any improvement. As the data rate increases, HPF becomes more efficient and at 10 Mbit/s the penalty is already very small. For higher data rates the penalty becomes quite small, even without HPF. The result of this behaviour is that systems operating at data rates around 10 Mbit/s are the most power efficient, for the same modulation scheme. For 10 Mbit/s, the use of 4-PPM requires only 0.6 dB more power than a system operating at 1 Mbit/s using 16-PPM. This result is relevant considering that 4-PPM is less sensitive to multipath dispersion than 16-PPM [1].

5.5 Discussion

The results presented suggest that if a system is to operate under artificial light interference several aspects have to be considered during the system design. If the interference produced by fluorescent lamps driven by electronic ballasts is not present, then any modulation method can be used, provided that highpass filtering is used. In this case, the power efficiency of L-PPM becomes even higher compared to that of OOK,

making L-PPM a good solution. This conclusion is valid for all the data rates considered in this paper. If however the system has to operate under the interference produced by fluorescent lamps driven by electronic ballasts, the results show that OOK is not a practical solution unless a different technique is used to combat the interference. In this case the best solution, in terms of power efficiency, seems to be to design the system to operate at a data rate around 10Mbit/s and adopt a 4 or 16-PPM modulation scheme depending on the amount of intersymbol interference introduced by multipath dispersion.

6 Conclusions

The performance of wireless infrared transmission systems operating under artificial light noise and interference was evaluated for systems using OOK-NRZ, L-PPM and BPSK modulation schemes, with and without electrical highpass filtering. The three types of artificial light interference were considered and results were presented for typical ambient light conditions derived from a statistical characterisation of the channel.

The major conclusion is that artificial light interference has to be considered in the evaluation of the system performance and in system design. For the interference produced by incandescent lamps and fluorescent lamps driven by conventional ballasts, small penalties are induced in L-PPM systems with MAP detection even without highpass filtering, while for OOK systems the large penalty induced by these types of interference can be effectively mitigated by resorting to electrical highpass filtering. The interference produced by fluorescent lamps driven by electronic ballasts induces severe power penalties in both OOK and L-PPM systems. For L-PPM, significant reductions on that penalty can he achieved by resorting to electrical highpass filters, while for OOK highpass filtering shows very little efficiency.

We have also observed that, as expected, the effects of the interference are more important for systems operating at low data rates. For OOK without high-pass filtering the optical power required for a given BER is almost independent of the bit rate within the range of interest.

7 Acknowledgments

The first author would like to thank Junta Nacional de Investigação Científica e Tecnológica for its financial support. This work is being carried out as part of the ITCOM - 'Integration of Technologies for Mobile Communications' project, commissioned by the program PRAXIS XXI.

8 References

1 KAHN, J.M., BARRY, J.R., AUDEH, M.D., CARRUTHERS, J.B., KRAUSE, W.J., and MARSH, G.W.: 'Non-directed infrared links for high-capacity wireless LANs', *IEEE Personal Commun.*, second quarter 1994, pp. 12–25

2 LOMBA, C.R.A.T., VALADAS, R.T., and DUARTE, A.M.O.: 'Propagation losses and impulse response of the indoor optical channel: a simulation package'. Proceedings of international seminar on *Digital communications*, Zurich, Switzerland, March 1994, (Springer-Verlag), pp. 285–297

3 MOREIRA, A.J.C., VALADAS, R.T., and DE OLIVEIRA DUARTE, A.M.: 'Characterisation and modelling of artificial light interference in optical wireless communication systems'. Proceedings of the sixth IEEE international symposium on *Personal, indoor and mobile radio communications* (PIMRC'95), Toronto, Canada, September 1995

4 GFELLER, F.R., BERNASCONI, P., HIRT, W., ELISII, C., and WEISS, B.: 'Dynamic cell planning for wireless infrared in-house data transmission'. Presented at the international seminar on *Digital communications*, Zurich, Switzerland, March 1994,

5 GFELLER, F.R., and BAPST, U.: 'Wireless in-house data communication via diffuse infrared radiation', *Proc. IEEE*, 1979, **67**, (11)

6 MOREIRA, A.J.C., VALADAS, R.T., and DE OLIVEIRA DUARTE, A.M.: 'Modulation/encoding techniques for wireless infrared transmission'. Submitted to IEEE 802.11 standardisation project, May 1993

7 CHEN, K.-C.: 'Direct detect modulations of high speed indoor diffused infrared wireless transmission'. Proceedings of the fifth IEEE international symposium on *Personal, indoor and mobile radio communications* (PIMRC'94), The Netherlands, September 1994

8 PAHLAVAN, K.: 'Wireless communications for office information networks', *IEEE Commun. Mag.*, 1985, **23**, (6)

9 MCCULLAGH, M.J., WISELY, D.R., EARDLEY, P.L., and SMYTH, P.P.: 'A 50 Mbit/s optical wireless LAN link using novel optical and electronic enabling technologies'. Presented at the 1994 international seminar on *Digital communications*, Zurich, Switzerland, 1994

10 TAVARES, A.M.R., MOREIRA, A.J.C., LOMBA, C.R.A.T., MOREIRA, L.M.V., VALADAS, R.J.M.T., and DE OLIVEIRA DUARTE, A.M.: 'Experimental results of a 1Mbps IR transceiver for indoor wireless local area networks'. Presented at the fifth international conference on *Advances in communication and control*, COMCON 5, Crete, Greece, 1995

11 MARSH, G.W., and KAHN, J.M.: '50-Mb/s diffuse infrared free-space link using on-off keying with decision-feedback equalization'. Proceedings of the fifth IEEE international symposium on *Personal, indoor and mobile radio communications* (PIMRC'94), The Hague, The Netherlands, September 1994, pp. 1086–1089

12 AUDEH, M.D., and KAHN, J.M.: 'Performance evaluation of baseband OOK for wireless indoor infrared LAN's operating at 100 Mb/s', *IEEE Trans.*, 1995, **COM–43**, (6), pp. 2085–2094

13 DE OLIVEIRA DUARTE, A.M., and VEIGA, G. (Eds.): 'Report EUR 14932 - WINS - wireless in-house network studies'. ESPIRIT PROJECT 5631, European Commission, 1994

14 PROAKIS, J.G.: 'Digital communications' (McGraw–Hill, 1989, 2nd edn.), Chap. 4, p. 248

15 IEC 825-1: 'Safety of laser products - part 1: Equipment classification, requirements, and user's guide'. International Electrotechnical Commission, 3 Rue de Varembé, CH - 1121, Geneva 20, Switzerland, 1993

16 SPW - Signal Processing WorkSystem is a registered trademark of the Alta Group of Cadence Design Systems Inc.

17 LOMBA, C.R.A.T., VALADAS, R.T., DE OLIVEIRA DUARTE, A.M.: 'Safety issues of the baseband IR PHY'. Submission to IEEE 802.11 standarisation project, August 1994